PERGAMON

Journal of Structural Geology 22 (2000) 1261–1283

JOURNAL OF STRUCTURAL GEOLOGY

www.elsevier.nl/locate/jstrugeo

# The geometry and kinematics of the Main Boundary Thrust and related neotectonics in the Darjiling Himalayan fold-and-thrust belt, West Bengal, India

Malay Mukul

*CSIR Centre for Mathematical Modelling and Computer Simulation, 560 037 Bangalore, India*

Received 9 June 1999; accepted 30 March 2000

**Abstract**

The Main Boundary Thrust (MBT) is well-exposed in a section of the Tista River valley in the Darjiling Himalayan fold-and-thrust belt. The fault trace trends E–W across the N–S flowing Tista and thrusts Gondwana (Permian) age sandstones over Lower Siwalik (Miocene) age sandstones. The MBT has been folded into a fault propagation synform–antiform pair by tectonic activity along a younger, South Kalijhora Thrust (SKT) in its footwall that transports Lower Siwalik rocks over Middle Siwalik sandstones; the SKT cuts through the fault propagation structure preserving the MBT fault–propagation fold pair in its hanging wall. The motion along the SKT rotated the bedding and the limbs of the folded MBT in its hanging wall. Footwall imbrication in front of the SKT further rotated the folded MBT. Footwall imbrication continued to about 30 km south of the study area in the Middle Siwalik and younger section. The region has been subsequently reactivated as evident from uplifted gravel beds and strath terraces along the folded trace of the MBT fault zone and also in the footwall of the SKT. The reactivation resulted in the formation of connective splays off the existing faults, probably forming horses of a connecting splay duplex in the subsurface within the Siwalik section. The motion along these splays passively folded overlying beds, and formed uplifted gravel beds and strath terraces along the local drainage. The rotations resulting from footwall imbrication and reactivated splays probably caused the southern limb of the fault propagation synform to become overturned. The duplexing also raised the river bed and arrested the flow of the River Tista causing the river to 'pond' and deposit its load, resulting in the formation of a bar upstream of the MBT trace. The tectonic reactivation of the area points to taper-building activities in a subcritical wedge probably in response to monsoon-induced excessive erosion in the middle of the Darjiling–Sikkim–Tibet Himalayan thrust wedge. 

## 1. Introduction

River morphology and sedimentology have been given much attention by geomorphologists, sedimentologists and civil engineers in order to understand different aspects of flowing rivers and the effect they have on the natural and human environment. Several workers (e.g. Tator, 1958; Welch, 1973; Adams, 1980; Russ, 1982; Burnett and Schumm, 1983; Nakata, 1989; Ouchi, 1985; Schumm, 1986; King et al., 1994; Valdiya, 1998 and references within) have recognised the importance of active tectonics as a factor influencing river morphology and sedimentology, and both experimental and field study of rivers in areas undergoing active tectonics have been carried out. However, in almost all of these studies, the response of the river to active tectonics has been studied mostly in terms of overall subsidence and uplift of the channel, and the response of the river to it in front of the exposed mountain front. Typically, in a forelandward-migrating fold-and-thrust belt, the active front, if any, occurs in front of the exposed mountain front and the active thrust faults are blind. Deformation related to active tectonics in these situations can only be recognised by the uplift or subsidence in alluvial tracts of land (most

*E-mail address:* mlym@cmmacs.ernet.in (M. Mukul).

0191-8141/00/$ - see front matter 
PII: S0191-8141(00)00032-8

commonly cited evidence for neotectonic deformation is the warping of alluvial terraces) that may or may not be entirely attributable to tectonic activity along blind thrust faults in the subsurface. Therefore, it might be useful to look at possible neotectonic activity within the exposed mountain front of reactivated fold-and-thrust belts like the Himalayan fold-and-thrust belt and try and correlate it with the geometry and kinematics of *exposed* faults.

This approach would require first looking at deformation structures in exposed rock outcrops on the banks of the river (e.g., fault, fold, fault-related folds, etc.), the lithologies that have been deformed, and the geometry and kinematics of the deformation struc-

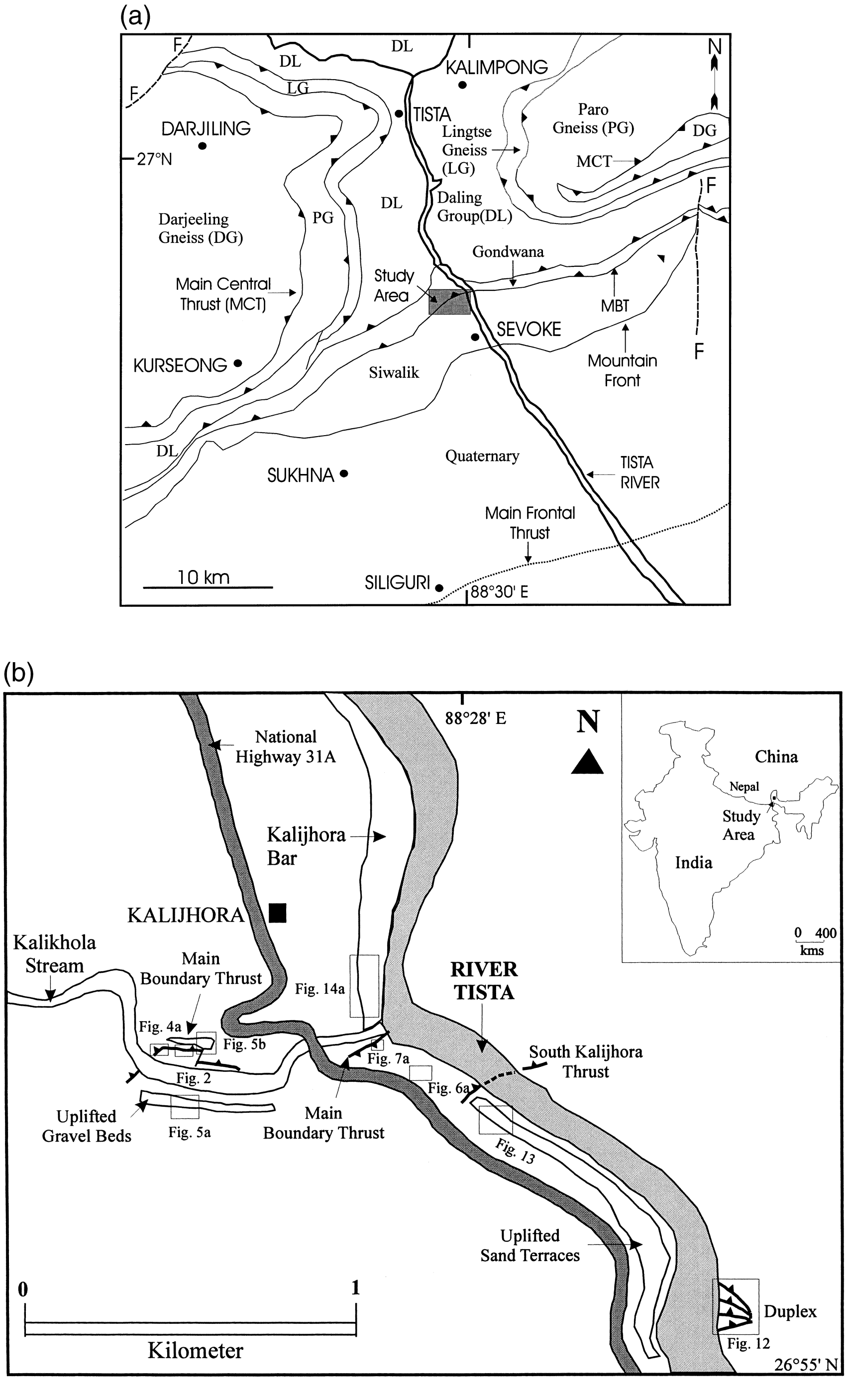


Fig. 1. (a) Regional structure of the Darjiling Himalayas (modified after Schwan, 1980). The study area has been boxed and details are shown in (b). The Main Frontal Thrust is buried and inferred to be located just south of the town of Siliguri on the basis of raised alluvium. (b) Map of the study area around Kalijhora town in the Darjiling Himalayas, West Bengal, India, with locations of the neotectonic features observed in the area. The geographic locations of photographs of geological features in the field that accompany this paper are indicated by rectangular boxes.

tures, followed by a study of how a river that cuts across the structures has been affected by it. This paper aims to present results of using this approach and carrying out an integrated study of the effects of active thrust tectonics near the Main Boundary Thrust (MBT) in the Himalayan orogen along stream sections parallel and perpendicular to the strike of the fault (Fig. 1b). The geometry and kinematics of the thrusting in the area are first worked out and then the effect on the local drainage is examined. This paper is based on studies carried out along the Tista and Kalikhola stream sections near Kalijhora town (26° 56′ 07″ N and 88° 27′ 10″ E) (Fig. 1b). The Kalikhola flows E–W in the study area and is a tributary of the N–S flowing Tista.

### 1.1. The River Tista

The River Tista is the main river in the Darjiling–Sikkim Himalayas (Fig. 1a). It is one of the most turbulent rivers in the Himalayas, mainly due to the steep topographic gradient found in the Darjiling–Sikkim Himalayas. Until 1787, the river flowed into the Ganges. However, it changed course subsequently and now empties into the Brahmaputra river. The Tista, like other major Himalayan rivers, is a trans-Himalayan river originating in northern Sikkim and flowing southwards toward the foothills.

The River Tista runs approximately N–S in the Darjiling Himalayas more-or-less parallel to the transport direction of the foreland thrust sheets of the Himalayan fold-and-thrust belt. This causes the river to cut across all the foreland thrust sheets in the area and be affected by motion (present and past) along these E–W striking thrusts. Flooding of the River Tista has been recognised near Kalijhora town (Fig. 1b) by Chakraborty and Chakraborty (1989), although it is not clear why the flooding occurred. This paper addresses this problem and attributes the flooding of the Tista in the above area to neotectonics involving the MBT and younger thrusts.

## 2. The Main Boundary Thrust

The term Main Boundary Thrust was introduced by Medlicott (1864) to define the faulted contact between the Siwalik and the older Murree (Miocene; Wadia, 1975) /Dharamshala (Oligocene to Early Miocene; Kumar, 1988) beds in the Himalayas of Jammu–Himachal Pradesh, India. In the Darjiling Himalayas the MBT has been described 'unambiguously' as the southern limit of the 'Main Himalayan structural units' (Roy, 1976; Acharyya, 1976). Using this definition, in Tista Valley, the MBT is considered to be the thrust that transports older, Gondwana (Permian,

Table 1
Stratigraphy exposed in the frontal Darjiling–Sikkim Himalayas[a]

| Age | | Stratigraphic unit | Name | Description |
|---|---|---|---|---|
| Cenozoic | Mio-pliocene | Upper Siwalik (400–500 m)[b] | Murti boulder bed | Crude bedded immature conglomerate |
| | | | Parbu grit | Pebbly sandstone and course medium sandstone |
| | | Middle Siwalik (800–1250 m)[b] | Geabdat sandstone | Medium- to course-grained sandstone and shale, local pebbly beds, minor marl |
| | | Lower Siwalik (200–250 m)[b] | Chunabati formation | Fine- to medium-grained sandstone, siltstone, claystone, marl |
| | | | | Basal conglomerate, Gondwana and older clasts of schists and slates |
| Paleozoic | Upper Permian | Gondwana group | Damuda subgroup | Sandstone, carbonaceous shale and coal |
| | Lower Permian | | Rangit pebble-slate (Talchir?) | Diamictite, rythmite, quartzite marl |
| Pre-Cambrian | | Daling Group | Buxa formation | Dolomites, fine-grained quartzites and pyritiferous shales |
| | | | Reyang formation | Variegated quartzites, shales and slates |
| | | | Gorubathan/Daling formation | Chlorite–sericite, greenish phyllites, quartzites and slates |
| | | | | Interbanded metabasics |

[a] After Acharyya (1994); Acharyya et al. (1976); Acharyya and Sastry (1976); Roy (1976); Schwan (1980).
[b] After Roy (1976).


Fig. 2. Exposure of the MBT fault zone along the north bank of the Kalikhola stream in the Darjiling Himalayas. The arrows point to the fault contact between the Gondwana Geabdat sandstones in the hanging wall and fault zone shales. A thin zone of cemented breccia is present along the contact zone. The hanging wall Gondwana sandstones dip gently to the north. A hammer is used for scale below the left arrow.

Damuda Subgroup) rocks from the north over the younger, Lower Siwalik (Miocene, Chunabati Formation) rocks to the south (Acharyya, 1976; Table 1). The MBT fault zone is exposed in the Kalikhola section south of the Kalijhora town in the Tista Valley (Fig. 1b; Acharyya, 1994).

### 2.1. Geometry of the Main Boundary Thrust

The MBT is exposed on the northern and southern banks of the Kalikhola stream. The trace of the folded fault zone runs approximately parallel to the E–W trace of the Kalikhola stream (Fig. 1b). The fault plane is exposed on the northern bank of Kalikhola and is defined by a thin, planar zone of fine-grained cemented breccia at the contact between the fault zone and hanging wall rocks and dips 50° towards 312° (Fig. 2). Coarse-grained Gondwana sandstone is present in the hanging wall of the MBT while a brecciated and fractured Gondwana sandstone–shale–coal sequence forms the partly exposed fault zone. Within the fault zone the bedding and the cleavage planes are sub-parallel to each other and dip dominantly to the northwest (Fig. 3). The hanging-wall Gondwana sandstones and the fault contact have been folded into an antiform around a north-easterly, gently plunging fold axis (Fig. 4); the limbs dip to the NW and SE. The Kalikhola stream flows across this antiformal hinge zone and changes its flow direction from N–S to E–W after crossing the hinge (Fig. 1b). Cleavage in the hanging-wall Gondwana sandstones is developed only in shaly intercalations within the Gondwana sandstones and is near vertical and steeper than bedding (Fig. 4b).

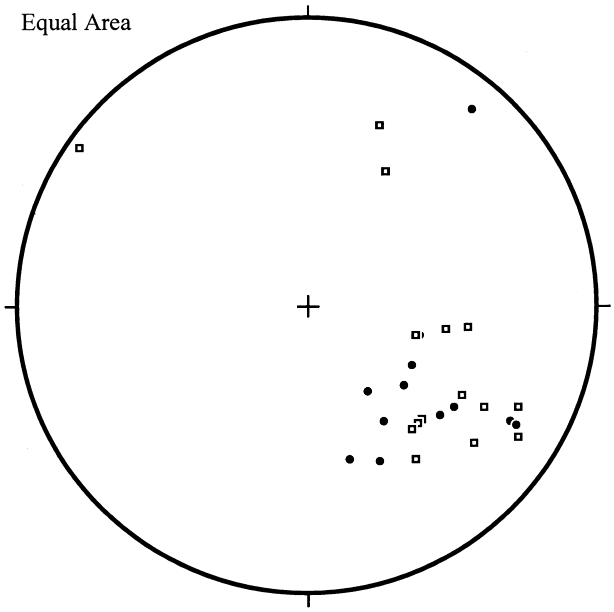


Fig. 3. Equal area stereoplot of poles to predominantly NW dipping bedding (●) and cleavage (□) in the shales and sandstones of the MBT fault zone seen in Fig. 2. Cleavage is observed to be sub-parallel to bedding in the fault zone.

Quaternary, unconsolidated gravels on the northern and southern banks of the Kalikhola have been uplifted by about 4 m relative to the present channel bottom near this location (Fig. 5a, b), defining strath surfaces and terraces. This suggests that they were uplifted either by very recent activity on the MBT or during the folding of the MBT fault zone. On the northern bank of the Kalikhola, the uplifted gravels were seen to directly overlie the north-westerly dipping fault zone rocks at one location (Fig. 5b). The gravels overlie the hanging-wall Gondwana rocks at other places thereby defining an irregular strath surface that cannot be used as a surface tilt indicator. The strath surface for the uplifted terrace on the southern bank of the Kalikhola (Fig. 5a) is not exposed. The uplifted gravels are overlain by soil and form terraces that are densely vegetated by grass and trees (Fig. 5). These strath terraces are very similar in height (above the

(a)


(b)

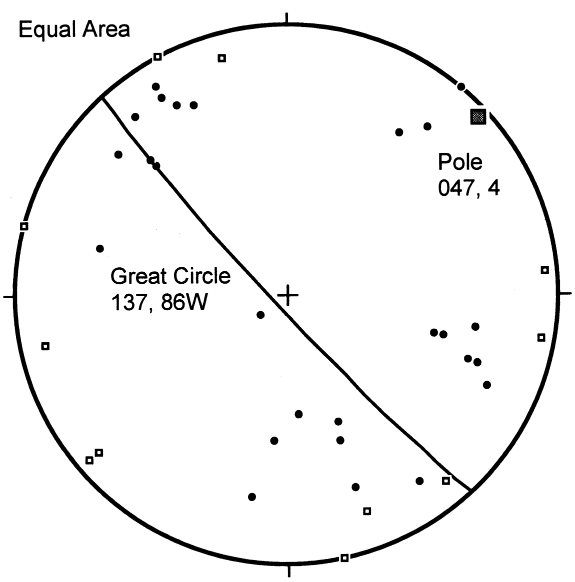


Fig. 4. Evidence of folding of the MBT fault zone along with the hanging wall Gondwana sandstones. (a) The fault contact (seen by the location of the hammer) and the hanging wall Geabdat sandstones dip southerly in this photograph as opposed to their NW dip seen in Fig. 2. (b) Equal area stereoplot of poles to bedding (•) and cleavage (□) in the hanging wall of the MBT in the Gondwana Geabdat sandstone along the northern bank of the Kalikhola section. Antiformal folding of the MBT fault zone and the hanging wall rocks around a north-easterly plunging fold axis is indicated by the plot.

present channel bottom) and extent of vegetation to terraces observed by Nakata (1989) on the banks of the Chel River along strike of the MBT east of the present study area close to the Indo-Bhutan border.

The entire MBT fault zone is exposed on the southern bank of the Kalikhola stream about 100 m west of the Kalikhola–Tista join (Fig. 1b). Acharyya (1976) described the MBT from this location. The footwall of the MBT here consists of Lower Siwalik sandstone that is folded into gentle, easterly plunging, antiforms and synforms (Fig. 6a, b). The hanging wall consists of the same coarse-grained Gondwana sandstone described in the hanging wall along the north bank of the Kalikhola (Fig. 2). The fault plane along the contact between the hanging wall and fault zone rocks dips SE (47°/123°) and is defined by fine-grained cemented breccia similar to that observed in the north bank section described above (Fig. 7a). The bedding and cleavage in the hanging-wall Gondwana sandstones dip to the south-east and are sub-parallel

(a)

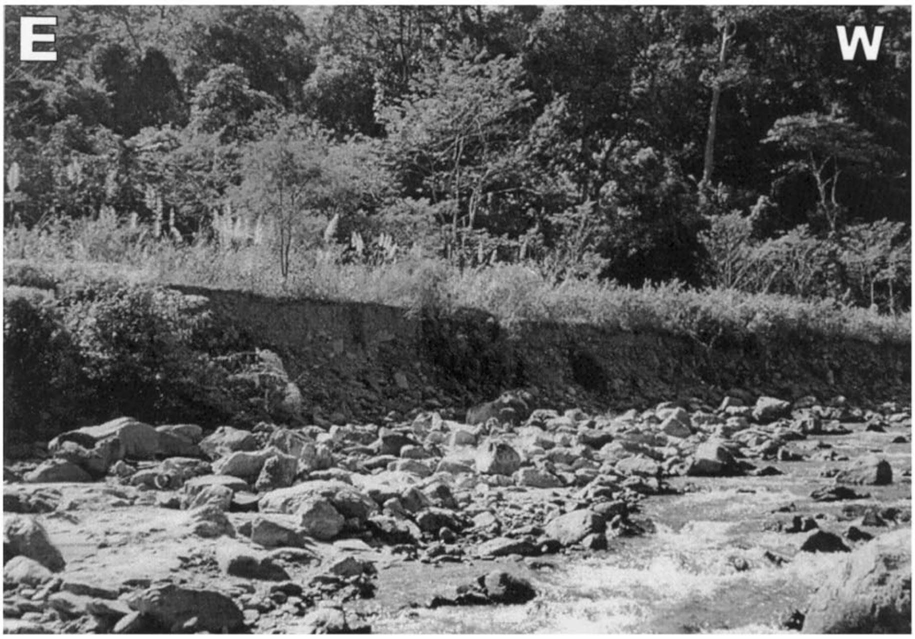


(b)


Fig. 5. Uplifted gravel beds along the south (a) and north (b) banks of the Kalikhola stream in the Darjiling Himalayas. The gravels uplifted along the south bank (a) form a terrace about 4 m above the present channel bottom, are overlain by soil and are densely vegetated by grass and trees. On the north bank (b) the uplifted gravels directly overlie the north-westerly dipping fault zone rocks over an irregular strath surface.

(Fig. 7b). Bedding and cleavage orientations within the fault zone are also subparallel and dip to the southeast (Fig. 8). It was not possible to work out for certain whether the cleavage was gentler than the bedding or vice-versa in the hanging wall or the fault zone because of their sub-parallel orientations. Bedding in the footwall immediately south of the MBT fault zone dips about 70–75° to the southeast. The structure exposed on the two banks of the Kalikhola (Fig. 9) can, therefore, be interpreted in two ways. First, given that the MBT fault zone exposed on the southern bank of the Kalikhola dips towards the south in the direction of the foreland, the older Gondwana sandstones are actually in the footwall of the fault (and the younger Lower Siwalik sandstones in its hanging wall) and the fault is a normal fault. If this is true then two faults must exist on the northern and southern banks of the Kalikhola. The NW-dipping fault plane exposed on the north bank of the river would be a thrust fault (MBT) with the coarse-grained Gondwana sandstone in the hanging wall and the SE-dipping fault plane exposed on the south bank would be a normal fault

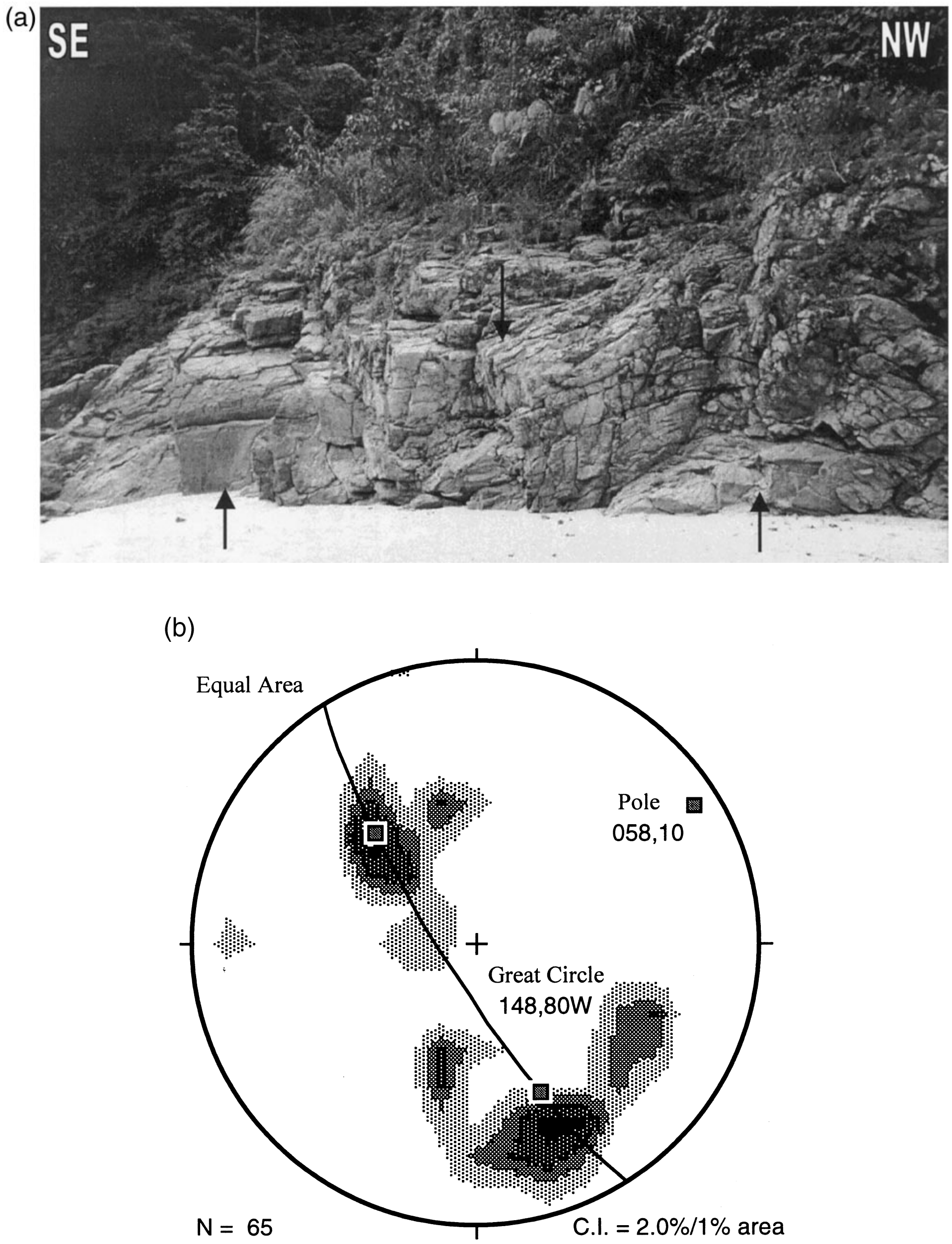


Fig. 6. Folding in the Lower Siwalik Chunabati Formation in the footwall of the MBT. (a) Gentle to open, upright, antiformal and synformal hinge zones, indicated by the arrows. The field of view is about 10 m across. (b) Stereoplot of poles to bedding in the Chunabati rocks in the footwall of the MBT. Folding along a NE-plunging axis is indicated.

with the coarse-grained Gondwana sandstone in its footwall (and Lower Siwalik rocks in the hanging wall). Alternatively, the MBT fault zone could also be interpreted as being folded; the south-dipping fault zone would then represent a fold limb. Given that no extensional features are observed within or outside the south-dipping fault zone, the antiformal folding of the MBT (Fig. 4), relative uplift of gravels and strath surfaces along the banks of the Kalikhola stream (Fig. 5), and the similarity of the fault zones exposed along both banks of the Kalikhola, the folded-fault hypothesis is favoured (Fig. 9).

The stratigraphy exposed in the hanging wall and footwall of the fault zones seen on the banks of the Kalikhola can be best explained by a synform–antiform fold pair (Fig. 9). The geometry of the antiform

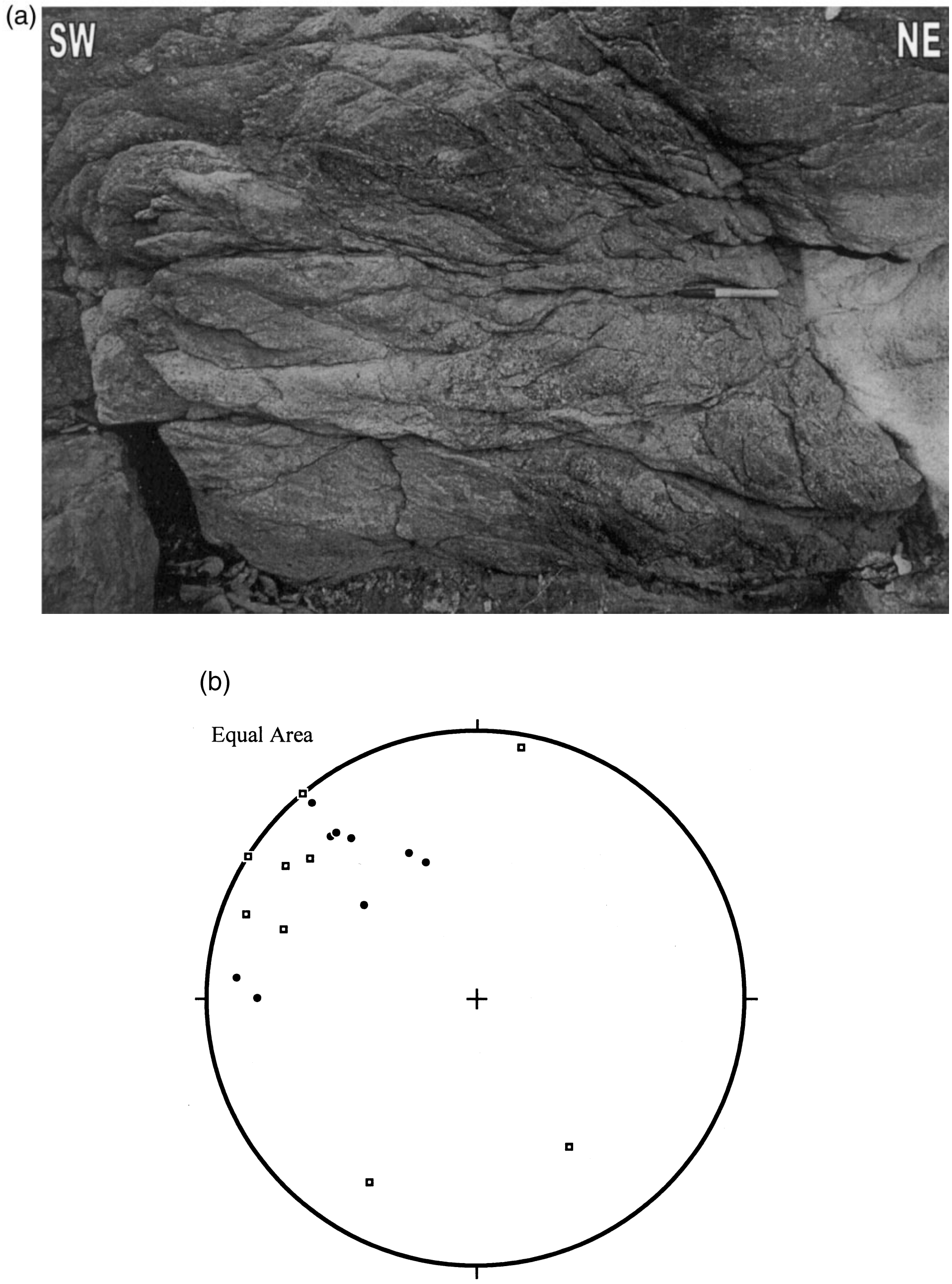


Fig. 7. (a) Fine-grained cemented breccia zone along the boundary of the MBT fault zone rocks and the hanging wall Geabdat sandstones observed along the southern bank of the Kalikhola stream section close to its junction with River Tista. The fault plane defined by the breccia is sub-parallel to the plane of the paper and the pen (scale) sits on it. The brecciated zone dips to the southeast indicating that the MBT fault zone is probably folded into an antiform–synform pair in which the synform is overturned and the antiform is not. (b) Equal area stereoplot of poles to bedding (●) and cleavage (□) within the MBT fault zone near the junction of Kalikhola stream and Tista River. The cleavage and bedding within the fault zone dip south-easterly and are sub-parallel.

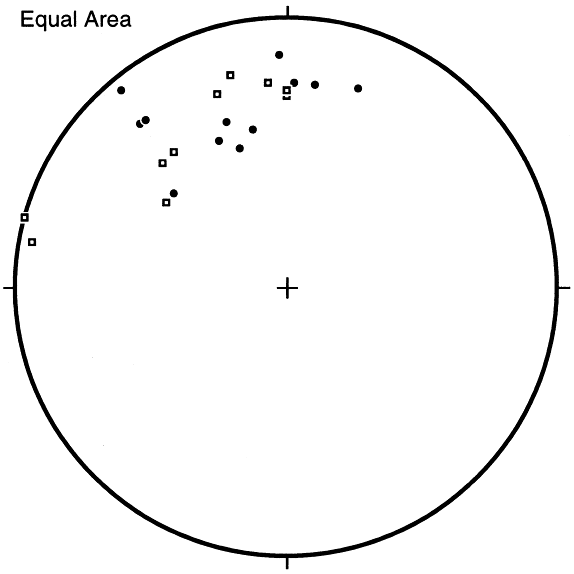


Fig. 8. Equal area stereoplot of poles to bedding (•) and cleavage (□) in the hanging-wall Gondwana sandstones of the MBT fault zone. Both the bedding and the cleavage within the fault zone dip moderately to the south-east near the junction between Kalikhola stream and Tista River and are sub-parallel (like the bedding and cleavage in the MBT fault zone and the breccia zone seen in Fig. 7).

has been deduced from field observations and data (Fig. 4). The south limb of the antiform dips to the southeast and must be the common limb of the antiform–synform fold pair. The south limb of the synform is exposed on the south bank of the Kalikhola stream and dips to the south-east like its north limb (Fig. 7). This indicates that the synform is an isoclinal fold (Fig. 9). Also, the cleavage and bedding orientations within the fault zone as well as the hanging wall rocks exposed along the south bank of the Kalikhola are sub-parallel to the fault zone boundaries. Such cleavage and bedding orientations are likely to develop on the limbs of isoclinal folds even if the cleavage is related to fault-parallel shear and is pre-tectonic to the folding. Syntectonic axial planar cleavage formed during the isoclinal folding, if any, is also likely to be sub-parallel to the bedding on the limbs of the isoclinal fold. The above discussion implies that both the fault zone and the hanging wall rocks have been folded into an antiform–synform pair; the synform, however, is overturned and the antiform is not (Fig. 9). This is an interesting geometry and the kinematics of its formation needs to be investigated in more detail.

### 2.2. Kinematics of deformation near the Main Boundary Thrust

The present geometry of the MBT and its hanging wall (Figs. 9 and 10e) is inferred to be an antiform–synform pair. This geometry indicates that the MBT was folded by slip along a younger thrust in its footwall. The South Kalijhora Thrust (SKT) that transports the Lower Siwalik Chunabati Formation and the MBT sheet over Middle Siwalik rocks, is the first footwall imbricate exposed in the footwall of the MBT. Fault-propagation folding and fault-bend-folding are two common mechanisms for formation of folds in fold-and-thrust belts. As fault-bend-folding involves passive folding of the thrust sheet over a ramp or a bend in the thrust carrying the sheet, a ramp in the SKT would be needed to fold the MBT in its hanging wall. Enveloping surfaces of the folds in the footwall of the MBT (Fig. 6) are sub-horizontal indicating that they are likely to overlie a flat in the SKT in the vicinity of the folding in the MBT. In fact, the SKT ramps upsection in the Lower Siwalik sandstones about half a kilometre south of the folded trace of the MBT (Fig. 10e) and is exposed along the western bank of the Tista. Also, fault-bend-folds usually result in open antiform–synform pairs which may get modified into overturned folds due to rotation along younger faults. However, it is unlikely that so much rotation can occur in a frontal or external thrust sheet due to motion along a fault in the Siwalik section; this is much more likely to happen in internal parts of a fold-and-thrust belt. On the other hand, overturned antiform–synform fold pairs are commonly associated with fault-propagation folds in fold-and-thrust belts (Mitra, 1990; McNaught and Mitra, 1993) and the motion along the South Kalijhora fault could easily have formed a fault-propagation-fold pair in front of the propagating thrust as a result of slower propagation rate of the thrust compared to the slip rate along it (Fig. 10b). In this interpretation, folding related to the propagation of the SKT folded the MBT, its hanging wall and its footwall. The SKT eventually cut through the fault-propagation structure (low-angle breakthrough; Mitra, 1990) preserving the fault-propagation-fold hinges in its hanging wall (Fig. 10c). Also, at this stage in the kinematic history of the region, the overall dip of the beds in the hanging wall of the SKT was northerly (Fig. 10c) as a result of rotation due to propagation and breakthrough of the SKT; this rotation also tightened the folds in the MBT.

Although detailed mapping of the area south of the SKT was beyond the scope of this study, more imbricate faults were observed during reconnaissance fieldwork in the region south of the SKT in the Middle Siwalik Geabdat sandstone unit. The Main Frontal Thrust (MFT) in the area is recognised by uplifted alluvial surfaces about 30 km south of SKT (Yeats et al., 1992; Valdiya, 1998) which indicates that frontal imbrication continued in front of the SKT. This implies that, by the Quaternary P, the active deformation front was likely to be at least 30 km south of

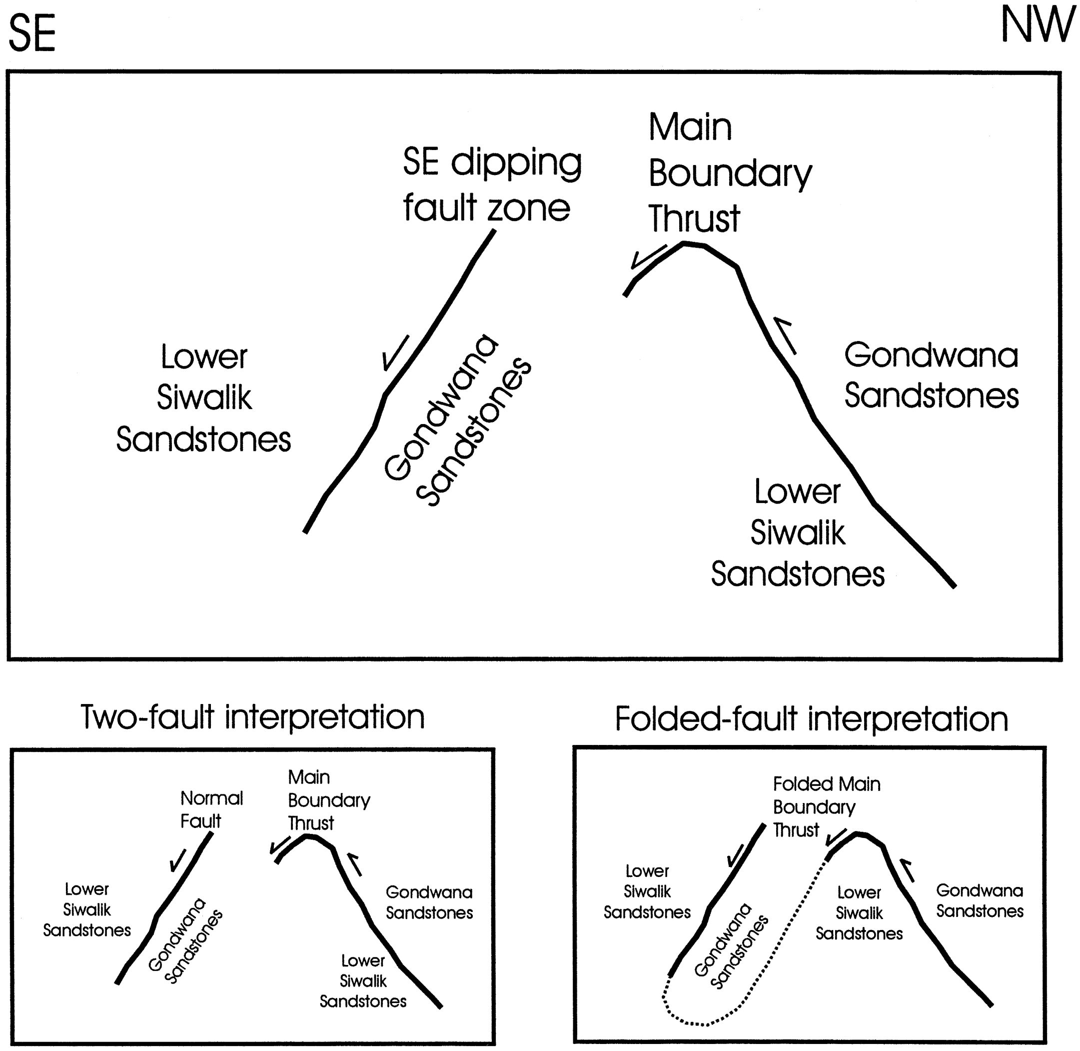


Fig. 9. Schematic sketch of the fault zone structures on north and south banks of Kalikhola and their possible interpretations. The folded-fault hypothesis is preferred here because of the antiformal folding of the fault zone observed in the field, absence of extensional structures, relative uplift of gravels and strath surfaces, and the similarity of the fault zones exposed along both banks of the Kalikhola.

the SKT if the usual hinterland to foreland succession of thrusting occurred in the Himalayan fold-and-thrust belt.

The important questions that need to be answered then include: why are Quaternary gravels being uplifted along the Kalijhora stream about 30 km north of the active deformation front? How may the open antiforms and synforms (Fig. 6) in the footwall of the MBT (or the hanging wall of the SKT) be explained? Finally, the geometry of the folded MBT and its hanging wall needs to be explained; specifically why the synform is overturned whereas the antiform is not (Figs. 9 and 10e). The model of the fault-propagation-folding that folds the MBT must explain both the isoclinal and overturned geometry of the synform and a more open and upright antiformal geometry.

To address the above questions, the footwall of the SKT was examined. Middle Siwalik Geabdat sandstone is exposed in the footwall of the SKT. Although there are no exposures of the Middle Siwalik rocks in the immediate proximity of the SKT on the west bank of the Tista, exposures on its east bank (which is inaccessible) indicate that the regional dip of the Middle Siwalik rocks in the footwall near the SKT is sub-horizontal. The footwall bedding steepens about a couple of kilometres away from the SKT and displays a northerly dip (Fig. 11) near the exposure of the Andherijhora Thrust which is the next footwall imbricate encountered south of (or in the footwall of) the SKT. The motion along this thrust may have also rotated the limbs of the folded MBT some more and tightened the folds further (Fig. 10d). A duplex consisting of three horses was also observed along the east bank of the Tista (Fig. 12) in the Middle Siwalik Geabdat sandstones in the hanging wall of the Andherijhora Thrust. The faults within the duplex are

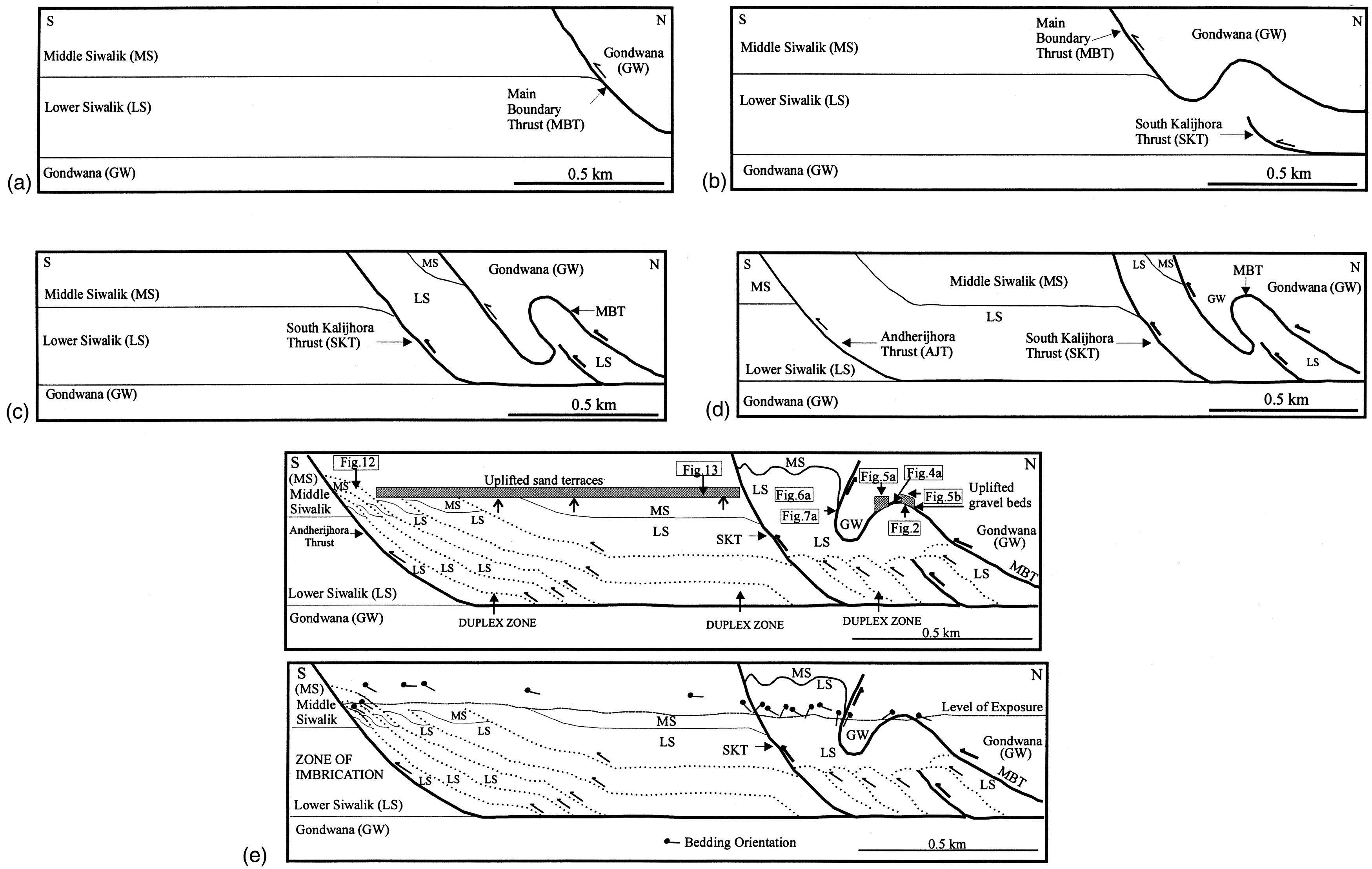


Fig. 10. Schematic diagrams explaining the kinematics of development of the fault and fold geometry observed near the Kalijhora region. (a) Deformation front is initially within the Gondwana section and the MBT is not folded. (b) Fault propagation folding in front of the propagating SKT folds the MBT and its hanging wall Gondwana rocks into an antiform–synform pair. (c) The SKT then cuts through the fault propagation structure preserving the related antiform–synform fold pair in its hanging wall. (d) This is followed by formation of a footwall imbricate (Andherijhora Thrust) in the footwall of the SKT. Imbrication continues in the footwall of the Andherijhora Thrust as far as the MFT which is located about 30 km south of the study area. (e) Fault splays join up with other splays or pre-existing faults to form horses of connective splay duplexes during rejuvenation in recent times. The geometry of the splays is not well-constrained and has, therefore, been drawn with dashed lines. Deformation associated with emplacement of different horses in the hanging wall of the SKT probably folds its hanging wall into upright antiform–synform fold pairs and also alters the geometry of the folded MBT and its hanging wall. The deformation also causes uplift of gravel beds along the Kalikhola section and the Tista River bed itself resulting in ponding of the Tista and the formation of Kalijhora bar. Deformation related to formation of a connective splay duplex in the hanging wall of the Andherijhora Thrust causes uplift of sand terraces on the west bank of the Tista.

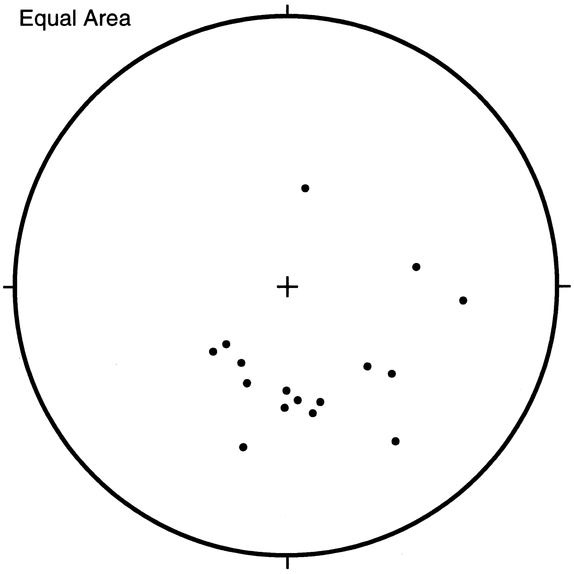


Fig. 11. Equal area stereoplot of poles to bedding (•) in the Middle Siwalik Geabdat sandstones in the footwall of the SKT near the exposure of the Andherijhora Thrust. The plot indicates that the most of the bedding dips are northerly.

present along the shaly bands within the Middle Siwalik sandstone. The bedding within the horses in the hanging wall of the Andherijhora Thrust dips to the north (Figs. 11 and 12) and the exposed horses occur immediately south of the sub-horizontal Middle Siwalik beds described above (Fig. 10e).

Several N–S trending river terraces were observed (Fig. 13) on the west bank of the Tista in the footwall of the SKT; the highest of these terraces occur almost 25–30 m above the water level in the present river channel. The terraces have also migrated successively from west (highest) to east (lowest) suggesting eastward migration of the river channel; the river flows directly in contact with the outcrops of Middle Siwalik rocks along its east bank between the exposures of the SKT and the Andherijhora Thrust (Fig. 12). The terraces are also asymmetric and observed only on the west bank of the river and occur only between the exposures of the SKT and the Andherijhora Thrust along the entire stretch of the Tista from the exposed mountain front (about 15 km south of the study area) to about 35 km north of it. Such localised occurrence of asymmetric river terraces indicates that local factors were responsible for their formation and preservation. These terraces were, therefore, studied in some detail to understand some of the factors responsible for their formation and preservation.

Asymmetric river terraces are observed in a N–S section near the exposure of the SKT (Fig. 13a, b). These terraces overlie the sub-horizontal beds of the Middle Siwalik rocks that are exposed on the east bank of the Tista. Terraces are defined by unsorted deposits of river sand and gravels (Fig. 13a) on sub-horizontal surfaces in the rock which may be bedding or strath surfaces cut by the river on the bedrock. The contact (strath surface) between the river deposits and the underlying bedrock is not exposed except for some isolated exposures of bedrock through the sand deposits (Fig. 13b). The sand and gravel deposits on each of these terraces is not more than a couple of metres thick. Given these characteristics of the river terraces observed along the west bank of the river Tista near the exposure of the SKT, they are interpreted as strath terraces rather than fill terraces. Five terraces were

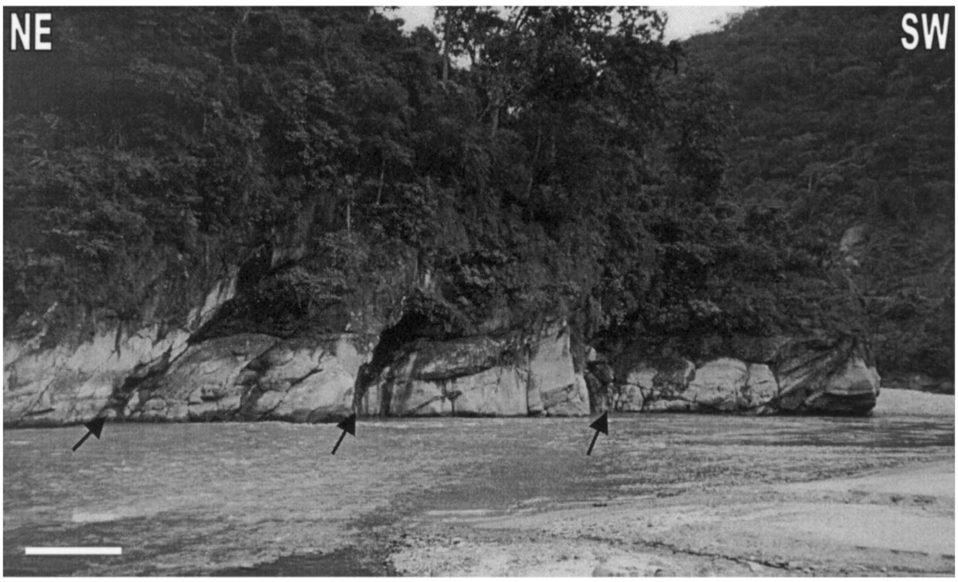


Fig. 12. Horses within the Geabdat sandstone in the footwall of the SKT defining a duplex. The fault planes (indicated by arrows) in the horses occur along shale horizons within the Middle Siwalik Geabdat sandstones. Scale bar = 15 m.

recognised in all. The highest terrace has developed a soil cover and is vegetated by thick bushes and some trees (Fig. 13c). The terrace beneath that is vegetated only by bushes and the lower terraces are either unvegetated or vegetated by only tufts of tall grass (Fig. 13b). Although there is no available information on the absolute ages of the formation of these terraces, the nature of their vegetative cover suggests that the higher, vegetated terraces were formed earlier and the lower unvegetated ones later.

River terraces and stream deposits can lie above an observed stream level due to a number of fluvial/hydrologic causes such as stream downcutting, drop in base level, rainfall or melt water increases. In the Himalayas, particularly, there is a considerable difference in monsoonal and non-monsoonal stream

(a)
(b)
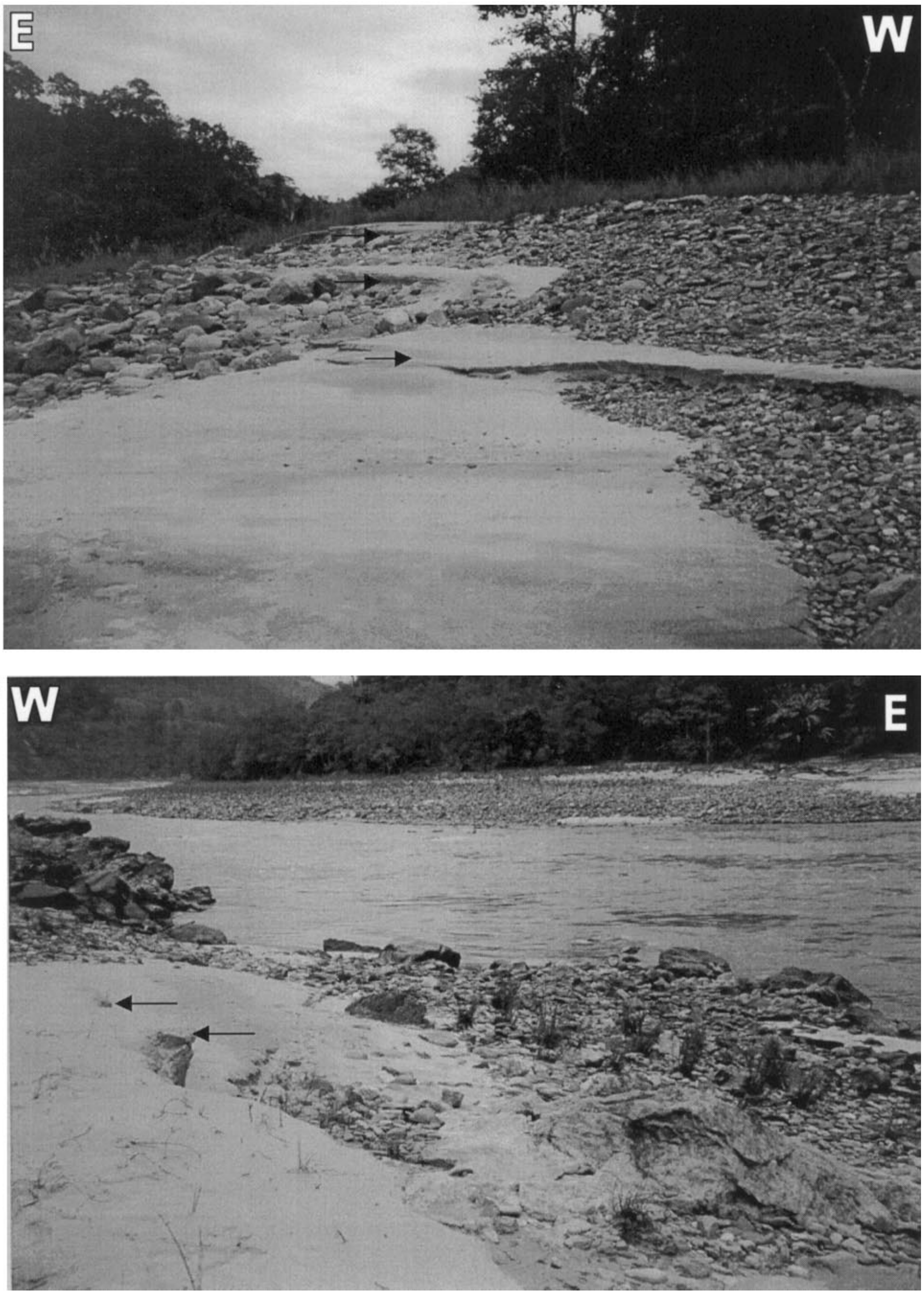


Fig. 13. Raised asymmetric, strath river terraces on the west bank of River Tista near the duplex seen in Fig. 12. (a) Three of the five terraces seen in the area are shown by arrows. Gravel that was part of the earlier bedload of the Tista and that has been left behind by the river as it adjusted to the uplift of the terrain is also seen. (b) Isolated exposures of Middle Siwalik sandstones under one of the strath terraces is shown by arrows. Tufts of grass represent the vegetation on a lower terrace. (c) Vegetation over a higher strath terrace (near the upper arrow in (a)). The uppermost terrace, shown by a horizontal arrow, is vegetated by thick bushes and trees. Progressive decrease of the extent of vegetation on these terraces indicate that the upper, more vegetated terraces were formed earlier than the lower less vegetated terraces.

(c)


Fig. 13 (*continued*)

levels. However, most of these factors are likely to have a regional impact on the flow of the river. Tectonic effects, if any, would be superposed on these fluvial/hydrological factors and cause localised deviations in geomorphologic features associated with regional river flow. Symmetric river terraces defined by sand deposits at about 2 m above the winter stream level are observed at many places along the length of the river within and outside the present study area. This regional river terrace is probably related to high monsoonal flow in the river. However, no river terraces 2–3 m above the winter stream level were observed anywhere outside the study area. This suggests that the strath terraces observed in the footwall of the SKT are local in extent and could be related to local increase in river downcutting rates and/or neotectonic uplift. Increased river downcutting rates could be a factor in the formation of the strath terraces in the footwall of the SKT because the Middle Siwalik sandstones are friable and more susceptible to river erosion than any other rock unit exposed in the study area. However, if increased river downcutting rate in the Middle Siwalik rocks was the primary factor in formation of these strath terraces, they would be expected to occur all along the river south of the SKT because the Middle Siwalik sandstone are exposed all the way from near the SKT to the exposed mountain front. That is not the case and, therefore, neotectonic uplift must be an important factor in the formation and preservation of strath terraces up to 25 m above the present stream level in the footwall of the SKT. This contention is also supported by the fact that these terraces only occur in the area between the SKT and Andherijhora Thrust and in close proximity of a duplex within the Middle Siwalik section in the hanging wall of the Andherijhora Thrust (Fig. 12).

If we accept that neotectonics did play a role in the formation and preservation of the strath terraces along the trace of the MBT and in the footwall of the SKT, we need to explain the neotectonics in the area both in terms of the kinematics of the faults observed in the area and the nature of the Himalayan wedge in the region. We will only discuss the neotectonics in terms of the faults observed in the area for now and take up the wedge scale deformation in a later section. Given that in a fold-and-thrust-belt inactive faults in the hanging wall of an active fault are likely to behave as passive markers and become folded by fault-related folds along with the rest of the hanging wall, it is unlikely that reactivation of MBT in the Quaternary was responsible for uplift of Kalikhola stream gravels and terraces along the MBT. Instead, Quaternary neotectonic activity in the footwall of the MBT is more likely to have caused the uplift. Quaternary reactivation of SKT and faults in its footwall (including the Andherijhora Thrust), therefore, may explain the raised strath terraces and stream gravels along the Tista and the Kalikhola. However, in the absence of any geochronological data on the movement along any of these faults, it is not possible to be certain about Quaternary reactivation of these faults in the Siwalik. The neotectonics of the area suggested above is also supported by some earthquake hypocenter data (Table 2) that indicate activity in the footwall of the MBT. We also have to keep in mind that the neotectonic activity described here is not taking place in front of the exposed mountain-front (e.g. Nakata, 1989) but within the mountains 30 km north of the exposed mountain front. This implies that we have to consider neotectonics in an area where pre-existing imbricate and folded thrusts are already present.

The kinematics in a region where previous thrusts exist is in itself an interesting puzzle. The most likely mechanism by which neotectonic deformation can occur in such a region is by the formation of splays off pre-existing thrust faults which join other splays or pre-existing faults to form horses, eventually constituting what is described as a connecting splay duplex (Mitra and Sussman, 1997). The deformation associated with duplex formation and the reactivation of the pre-existing thrusts can give rise to an overall uplift of the area; sub-horizontal beds above the horses and splays are likely to become folded passively into open, upright antiforms and synforms (e.g. Srivastava and Mitra, 1994) and pre-existing fold geometries are likely to be modified. The neotectonics observed in the study area is interpreted to be related to the formation of connective splays in the footwall of the MBT and the SKT, and three-horse duplex observed in the footwall of the SKT is interpreted as a connective splay duplex. Quaternary reactivation of SKT and the Andherijhora Thrust may also be a part of the process; the kinematics can be constrained further only when data related to the timing of motion on the different faults in the area become available.

Formation of connective splays in the subsurface (footwall) of the folded MBT are also a likely mechanism for the rotation of the overturned limb of the fault propagation antiform–synform fold which folds the MBT. The effect of splay-induced rotation of the overturned limb of the fault propagation fold is to make the antiform open and upright and the synform overturned; the overturned limb of the synform dips to the south after the rotation. This rotation would also be likely to uplift the gravels along the Kalikhola stream that were deposited over the antiformal hinge prior to the rotation of the overturned fold limb (Fig. 10e); gravel beds overlying the antiformal hinge zone were uplifted vertically and formed terraces (Fig. 5). It can also be argued that the upright folds in the Chunabati formation of the South Kalijhora sheet (Fig. 6) were formed by passive folding of the overlying beds above the connective splay duplex in the hanging wall of the SKT (Fig. 10e). Alternatively, rotation related to the propagation and the breakthrough of the SKT (Fig. 10c) could have caused the folding of the Lower Siwalik rocks and the overturning of the synform as-

Table 2
Thrust-related earthquake hypocenter data from the area near the exposure of the MBT in the Darjiling–Sikkim Himalayas[a]

| Year | Date | Time | Latitude (north) | Longitude (east) | Depth (km) | Magnitude | Magnitude type |
|---|---|---|---|---|---|---|---|
| 1842 | 18 SEP | – | 27.00 | 88.30 | – | – | – |
| 1843 | 10 OCT | – | 27.00 | 88.30 | – | – | – |
| 1852 | MAY | – | 27.00 | 88.30 | – | – | – |
| 1862 | 18 JUN | – | 27.00 | 88.30 | – | – | – |
| 1863 | 29 MAR | – | 27.00 | 88.30 | – | – | – |
| 1863 | 08 JUL | – | 27.00 | 88.30 | – | – | – |
| 1863 | 11 AUG | – | 27.00 | 88.30 | – | – | – |
| 1863 | 21 AUG | – | 27.00 | 88.30 | – | – | – |
| 1863 | 17 OCT | – | 27.00 | 88.30 | – | – | – |
| 1864 | 30 AUG | – | 27.00 | 88.30 | – | – | – |
| 1865 | 09 SEP | – | 27.00 | 88.30 | – | – | – |
| 1865 | 16 NOV | – | 27.00 | 88.30 | – | – | – |
| 1865 | 16 DEC | – | 27.00 | 88.30 | – | – | – |
| 1869 | 21 MAR | – | 27.00 | 88.30 | – | – | – |
| 1869 | 23 MAR | – | 27.00 | 88.30 | – | – | – |
| 1869 | 09 JUN | – | 27.00 | 88.30 | – | – | – |
| 1869 | 09 AUG | – | 27.00 | 88.30 | – | – | – |
| 1875 | 26 APR | – | 27.00 | 88.30 | – | – | – |
| 1899 | 25 SEP | – | 27.00 | 88.30 | – | – | – |
| 1949 | 27 FEB | – | 27.00 | 88.30 | – | – | – |
| 1972 | 06 NOV | 10:56:13.53 | 26.8771 | 88.426 | 59.1 | 4.4 | Body wave (Mb) |
| 1972 | 06 NOV | 10:56:08.80 | 26.958 | 88.708 | 33.48 | 4.8 | Mb |
| 1986 | 01 JULY | 20:20:01.68 | 26.93 | 88.325 | 69.60 | 5.0 | Mb |
| 1988 | 27 MAR | 05:56:29.81 | 27.0843 | 88.4203 | 70.3 | 4.1 | Mb |
| 1996 | 23 MAR | 16:07:29.60 | 26.95 | 88.50 | – | 3.8 | Mb |
| 1996 | 13 SEP | 03:41:08.60 | 27.0330 | 88.2340 | 33 | 4.5 | Mb |

[a] Compiled from: http://www.isc.ac.uk/; http://quake.geo.berkeley.edu/ and http://wwwneic.cr.usgs.gov/.

sociated with the folded MBT. Again, the formation of connective splays in the footwall of the SKT and the formation of the connective splay duplex (Fig. 12) is interpreted to be responsible for the raised strath terraces (Fig. 13) observed in the footwall of the SKT. The difference in the amount of vegetation and soil cover that has developed on these terraces probably indicates that neotectonic activity has continued over some time; dating of these terraces would help constrain the time period through which the neotectonic activity has persisted.

## 3. Neotectonically induced flooding of the River Tista

Formation of connective splays in the hanging wall of the SKT (Fig. 10e) caused uplift of gravel along the banks of the Kalikhola stream to form E–W-trending strath terraces (Fig. 5a) and is responsible for the folding of its footwall (Fig. 6). The river bed of the N–S-flowing Tista is also likely to be affected by this uplift (near its intersection with the trace of the MBT (Fig. 1)) provided the uplift rate of the bed exceeds the erosion rate. If the river bed is raised above the water level due to the uplift, the river is dammed and ponding will result upstream of the flow-barrier. If the river bed remains below the water level during the uplift, the river flow is likely to be partially blocked and flow velocity upstream of the barrier will decrease. The river would still flood upstream of the barrier resulting in a pond (King et al., 1994; Molnar et al., 1994). Alternatively, if little or no ponding actually occurred and the same amount of water was flowing through reduced space over the barrier, the water velocity would need to increase over the barrier. Creation of a pond upstream of the barrier is likely to result in the deposition of the load (probably as a bar) carried by the river, depending on how much the flow-velocity is reduced behind the barrier. However, if the erosion rate of the river bed is close to its uplift rate, no barrier to the flow would be formed and the flow in the river will not be obstructed. Erosion rates may be close to uplift rates in situations where the river bed is uniform and consists of unconsolidated sediments, such as south of the Himalayan mountain front. However, within the mountain front, footwall and hanging wall lithologies change across fault zones exposed along river beds and may have varying degrees of susceptibility to erosion. In situations where more resistant rocks (such as quartzite) occur along the river bed and are uplifted due to neotectonic faulting or folding, it is more likely that erosion rates

(a)

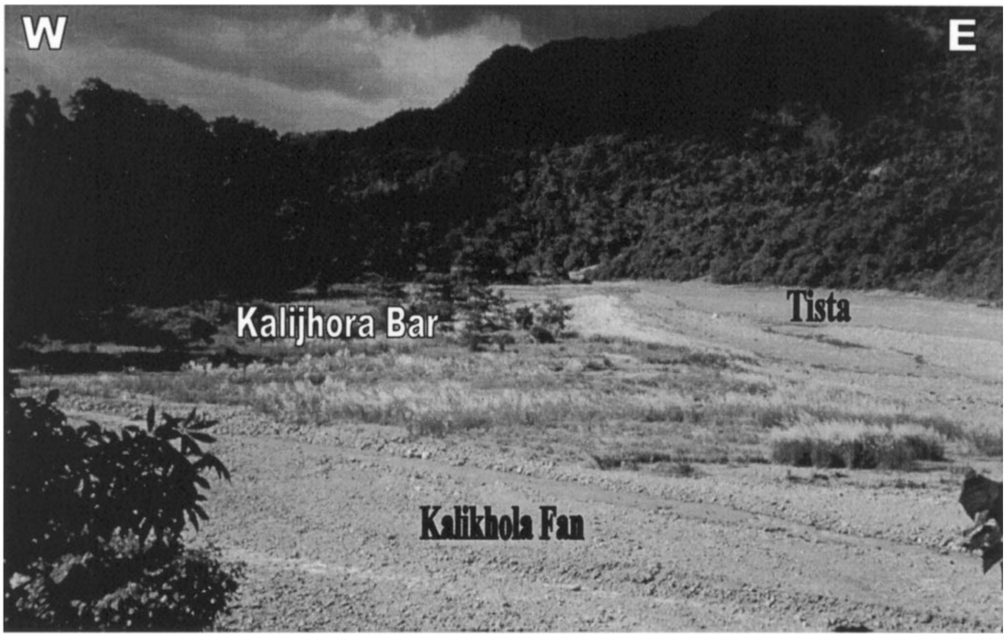


Fig. 14. (a) Photograph of the Kalijhora bar (Chakraborty and Chakraborty, 1989) near the join of Tista and Kalikhola streams. Most of the Kalijhora bar has been vegetated by bushes and trees. Unvegetated fan deposits consisting of cobbles and pebbles brought down by Kalikhola stream can be seen in the foreground. (b) Topographic map of the Kalijhora bar (modified after Chakraborty and Chakraborty, 1989) showing sediment distribution and elevation contours in metres relative to the present water level. The bar is about 9–10 m above the current water level near its outer edge. The Kalikhola fan deposits are elevated relative to the bar. (c) Sediments and sedimentary structures observed near the outer edge of the Kalijhora bar (after Chakraborty and Chakraborty, 1989). An overall upper-flow regime, interrupted by a period of lower-flow regime, is indicated by the deposits and the sedimentary structures; the lower-flow regime deposits could reflect ponding of the Tista in response to neotectonic uplift of its river bed along the trace of the MBT and the folding of its footwall.

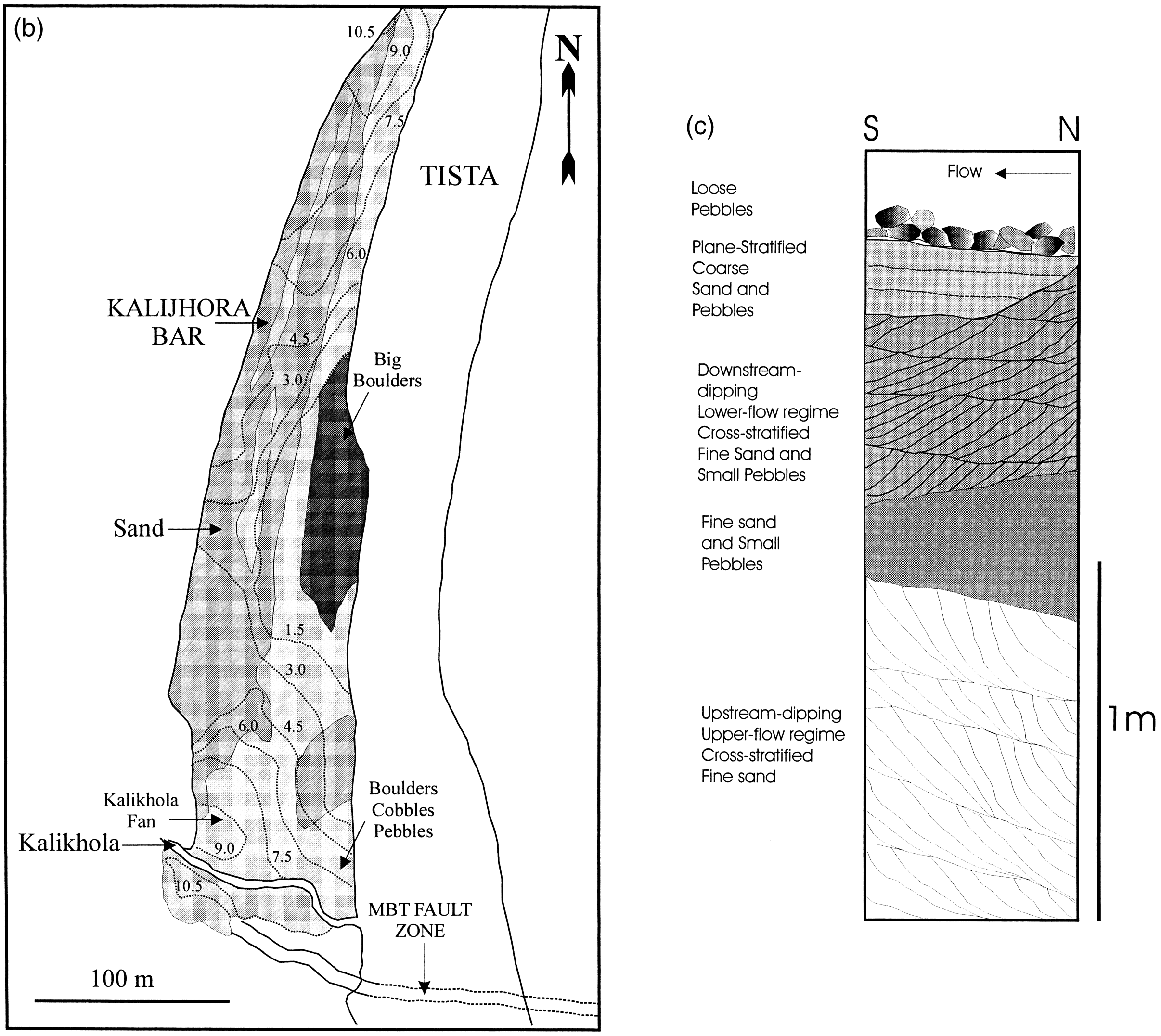


Fig. 14 (*continued*)

will be lower than the uplift rates, resulting in uplifted river beds that form a barrier to flow.

A 1.83-km-long bar named Kalijhora Point Bar (Chakraborty and Chakraborty, 1989), is exposed just upstream of the exposures of the Chunabati sandstones that occur in the footwall of the MBT (Figs. 1 and 14a). Although the river curves around Kalijhora town (Fig. 1b), the maximum thickness of the Kalijhora bar occurs along the straight stretch of the river following the bend. That is hard to explain purely in terms of the river hydraulics related to a bend in a river and the formation of bend-related point bars. Therefore, the deposition of sediments in the Kalijhora bar may be tectonically induced. Chakraborty and Chakraborty (1989) attributed the formation of the bar to probable local flooding of the Tista but did not suggest an origin for the flooding.

The sediments that are deposited in the bar exhibit unusual characteristics. The overall flow regime represented by deposits in the Kalijhora bar point to an upper flow regime (Chakraborty and Chakraborty, 1989). A traverse from the present water level to the edge of the hill slope reveals boulders near the water edge followed by a mixture of boulders, cobbles and pebbles, coarse sand with pebbles and fine sand (Fig. 14b). Decrease in grain-size in the bar sediments away from the present channel of the river suggests a decrease in the competency or the transporting ability of the river which in turn implies decrease in the flow velocity away from the main channel of the flooded river. The height of the bar near its outer edge is about 10 m above the present water level (Fig. 14b). Near the outer edge of the bar, fine sands with upstream-dipping foresets (antidunes of upper flow regime) are overlain by fine sands with small pebbles and downstream-dipping foresets (cross-stratification from lower-flow regime) in cross-section (Fig. 14c). Also, sands containing this lower-flow regime cross-stratification taper out about 500 m upstream of the trace of the MBT, suggesting that the lower-flow regime in the Tista was local and confined to the region immediately upstream of the MBT. These lower-flow regime sands are, in turn, overlain by upper-flow regime coarse sands and pebbles that exhibit planar stratification (Fig. 14c) indicating that a higher-flow regime returned subsequent to the lower-flow regime conditions.

The observations made above indicate that the Tista probably flooded over a period of time resulting in a gradual reduction of its flow velocity as indicated by the presence of lower-flow regime sands over the higher-flow regime sands at the base of the observed section (Fig. 14c). Presence of fine sand along the outer edge of the bar suggests that the stream velocity was lowest there although not low enough for silt to be deposited. This implies that the flow of the river was not blocked completely and, consequently, the river bed was probably not raised above the water level. Also, the fact that higher-flow regime sands overlie the lower-flow regime sands (Fig. 14b) near the top of the section indicates that the velocity of the stream increased gradually over a period of time as the flow-barrier was eroded down or the water level in the reservoir was raised above the height of the flow-barrier.

The question that needs to be revisited at this point is why was the river flooded in this manner over such a localised area. The Tista at Kalijhora is still very much within mountainous country characterised by high gradients and flow velocities and has not left the mountain front. As the MBT cuts across the river just downstream of the bar, it is conceivable that the folding of the MBT (Fig. 9) and the footwall Chunabati sandstones along E–W-trending fold axes (Fig. 6) by connective splays off pre-existing thrusts (and possible reactivation of older thrusts) also folded and uplifted the river bed of the N–S-flowing Tista, partially blocking its flow. This was also facilitated by the fact that the Lower Siwalik sandstones are more compact and hence more resistant to erosion than the Gondwana sandstones. This caused local flooding and ponding of the river and reduction of flow velocity that resulted in the deposition of the sediment load carried by the Tista and the formation of the Kalijhora bar.

## 4. Implications for wedge-scale tectonics

To understand the implications of the neotectonics within the Darjiling–Sikkim–Tibet wedge described above we will first look at the overall nature of the wedge on the basis of available data.

### *4.1. The Darjiling–Sikkim–Tibet Himalayan wedge*

Project INDEPTH (Nelson et al., 1996; Brown et al., 1996) gave the first insight into the deep level structure of the Himalayan hinterland in Tibet directly north of the Darjiling–Sikkim Himalayan fold-and-thrust shown in Fig. 1(a). A regionally developed, weak, mid-crustal partial melt layer under the Tibetan Plateau was imaged; it was postulated that the essential flatness of the Tibetan Plateau was caused by this layer because of the regional decoupling of the upper crust of the Tibetan Plateau from the lower crust and mantle lithosphere (Fig. 15). The INDEPTH images of the deep structure in the Higher Himalayas (Tethyan Belt) reveal a ramp in the basal detachment of the Himalayan fold-and-thrust belt (MFT) at a depth of

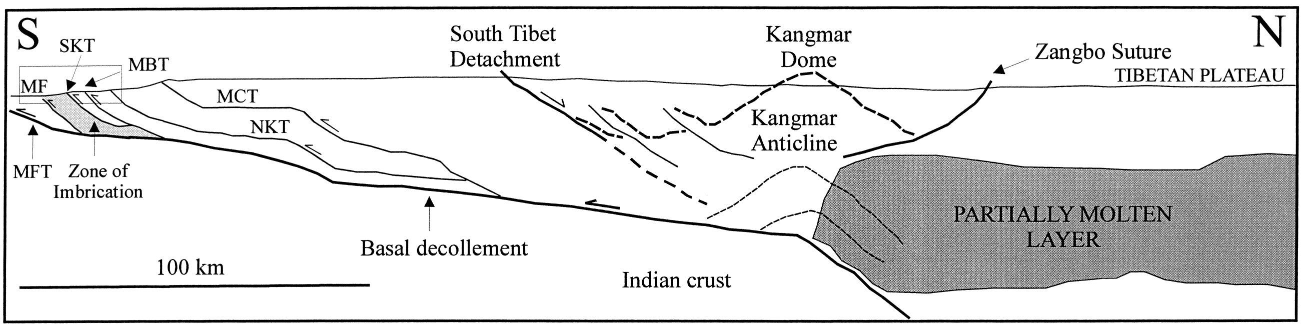


Fig. 15. Large-scale structure of the Darjiling–Sikkim–Tibet Himalayan wedge (after Acharyya, 1994; Nelson et al., 1996). The Kangmar Dome is the surface expression of the large-scale, basement-cored, ramp anticline that developed over a ramp in the basal detachment of the wedge at about 70-km depth. The formation of the Kangmar structure resulted in an initial, supercritical, taper and caused the Kangmar anticline to be the initial dominant hinterland structure that drove the frontal folding and thrusting in the wedge. Supercritical taper was also probably reduced by hinterland collapse by normal faulting along the South Tibetan Detachment (STD) system. The boxed area points to the coverage of Fig. 16. Abbreviations: MFT—Main Frontal Fault; MF—Mountain Front; SKT—South Kalijhora Thrust; MBT—Main Boundary Thrust; NKT—North Kalijhora Thrust; MCT—Main Central Thrust.

about 70 km and an associated basement-cored ramp antiform [the Kangmar Dome; Nelson et al., 1996 (Fig. 15)]. This antiformal structure is responsible for the high topographic elevation (> 3 km elevation) and relief of the Tethyan belt in Tibet north of the Darjiling–Sikkim Himalayan fold-and-thrust belt. It is conceivable from the scale of the Kangmar structure, its association with a ramp along the basal detachment in the Himalayas (Main Himalayan Thrust), and its proximity to the Zangbo Suture (Fig. 15) that it formed very early in the history of Himalayan tectonics probably during or just after the initial collision (probably Early Eocene) of the Tibetan and Indian plates. Valdiya (1998) talks about collision and welding of India and Asia between ~65–55 Ma followed by 'ridging up' of Asia–India junction around 50 Ma in the hinterland of the Kumaon and Garhwal Himalayan fold-and-thrust belt; this 'ridging up' event may indicate the formation of structures similar to the Kangmar antiform in the hinterland of the Kumaon and Garhwal Himalayas. It is also evident from the amplitude (c. 40 km) of the basement-cored Kangmar antiform (Nelson et al., 1996) that the formation of the structure will create an initial, supercritical taper in the hinterland of the Sikkim–Darjiling fold-and-thrust belt. The Kangmar structure would then serve as the 'dominant hinterland structure' (DeCelles and Mitra, 1995) that would drive the deformation in the frontal part of the Darjiling–Sikkim Himalayan fold-and-thrust belt.

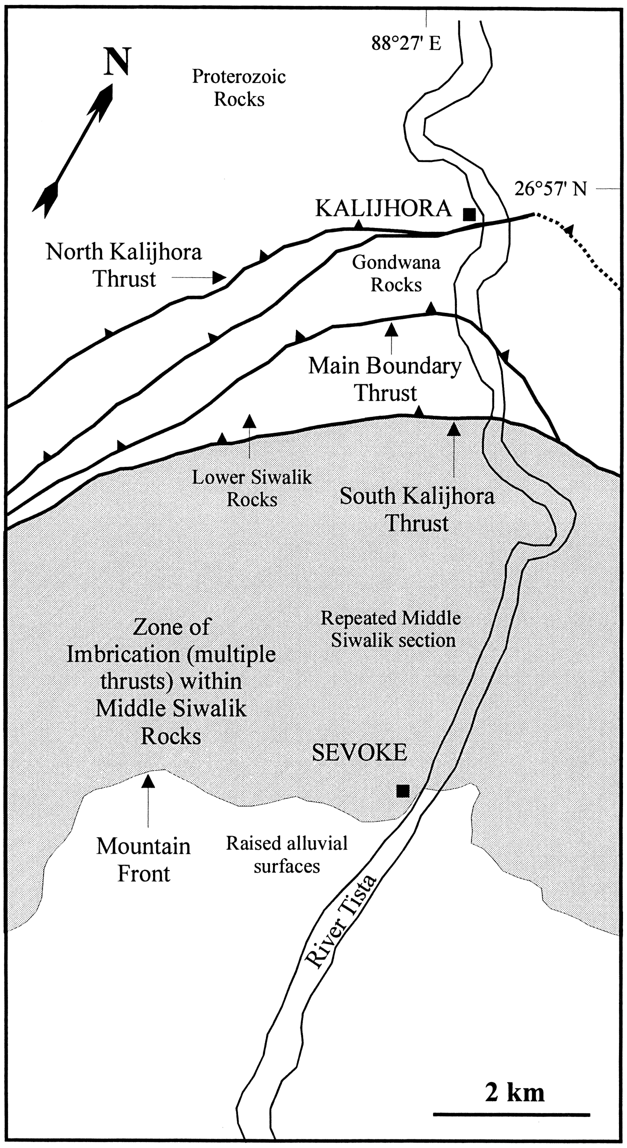


Fig. 16. Frontal imbrication in the Darjiling–Sikkim–Tibet Himalayan wedge south of the MCT (modified after Acharyya, 1994). At least three major imbricate thrust faults and a zone of imbrication in the Middle Siwalik section exist in the frontal part of the wedge (boxed area in Fig. 15) which points to the probable existence of supercritical taper at the back-end of the wedge that was created by the formation of the Kangmar structure. The MFT is blind in the region as evident from uplifted alluvial surfaces south of the mountain front.

In accordance with the critical wedge theory (Chapple, 1978; Elliott, 1976; Davis et al., 1983; Dahlen, 1984; Stockmal, 1983; Emmerman and Turcotte, 1983; Willett, 1992; Williams et al., 1994; DeCelles and Mitra, 1995; Boyer, 1995; Mitra, 1997 and as applied to the Himalayas, Mugnier et al., 1994 and Chalaron et al., 1995), the supercritical Darjiling–Sikkim–Tibet Himalayan wedge would need to lose taper by frontal imbrication and/or hinterland collapse. The South Tibetan detachment system (STD) is composed of several normal faults (Fig. 15) and probably indicates hinterland collapse of the sediments overlying the basement core of the Kangmar antiform. As the details of the deformation in the central part of the Darjiling–Sikkim–Tibet wedge are yet to be worked out (ongoing work) on the basis of modern concepts in fold-and-thrust geology, it is difficult to gauge the details of deformation in the wedge at the present time. However, the frontal part of the Darjiling–Sikkim–Tibet wedge reveals extensive frontal imbrication south of the Main Central Thrust (MCT).

Thrust faults in the Darjiling–Sikkim Himalayas have not yet been dated. Dates on the thrusts from other parts of the Himalayas (e.g. Kumaon and Garhwal Himalayas; Raiverman, 1997) do not seem to establish conclusively either the evolutionary model of Le Fort (1975), Lyon-Caen and Molnar (1983), Molnar (1990) and Valdiya (1998) that postulates successive development of Himalayan thrusts from north to south or the steady-state model of Powell (1979), Seeber and Armbruster (1981), Ni and Barazangi (1984) that postulates simultaneous activation of detachment thrusts of MCT, MBT and MFT. In the absence of dates on the motion along the various thrusts in the

Darjiling–Sikkim Himalayas, an initial north-to-south succession (evolutionary model) of thrust fault formation in the area is assumed. This is because modern fold-and-thrust geology postulates an initial hinterland to foreland succession of imbricate fault development (Dahlstrom, 1970; Boyer and Elliott, 1982). Thus, the MCT is likely to be the first frontal imbricate in the Darjiling–Sikkim–Tibet wedge that reduced the supercritical taper generated in the wedge as a result of the formation of the Kangmar antiform. South of the MCT, the North Kalijhora Thrust (NKT) carried Proterozoic sediments over Gondwana rocks (Table 1) and was probably the next major frontal imbricate that developed (Figs. 15 and 16) although there are intraformational thrust faults present within the Proterozoic section between the MCT to the north and the NKT to the south. It is not clear at this point if these intraformational thrust faults are out-of-sequence faults or not. The next major frontal imbricate to develop south of the NKT was the MBT (Acharyya, 1994) which carried Gondwana rocks (Table 1) over the Lower Siwalik rocks (Figs. 15 and 16). Frontal imbrication continued south of the MBT in the Siwalik section; the SKT carried Lower Siwalik rocks over Middle Siwalik sandstones (Table 1) and shales (Fig. 16). South of the SKT, frontal imbrication continued in the Middle Siwalik section and repeated the Middle Siwalik section several times (Acharyya, 1994; Fig. 16). The MFT is blind in this region as evident from uplifted alluvial surfaces south of the mountain front that is defined by the southernmost imbricate within the Middle Siwalik section (Fig. 1a).

The frontal imbrication pattern observed in the Darjiling–Sikkim–Tibet wedge indicates that at least four major thrust faults and a zone of imbrication (in the Middle Siwalik section) exist in the frontal part of the Darjiling–Sikkim–Tibet wedge (Figs. 15 and 16). This points to the existence of supercritical taper in the hinterland of the Darjiling–Sikkim–Tibet wedge because footwall imbrication in the front of the wedge is a mechanism by which a supercritical wedge reduces taper (Boyer, 1995; Mitra, 1997). It appears that both extensive frontal imbrication as well as hinterland collapse by normal faulting along the STD detachment system (Fig. 15) combined to reduce the initial supercritical taper generated by the formation of the Kangmar basement-cored antiform. Therefore, it is apparent that the Kangmar antiform in the Tibetan Higher Himalayas was the dominant hinterland structure that drove the foreland folding-and-thrusting in the Darjiling–Sikkim Himalayan fold-and-thrust belt.

### *4.2. Implications of the neotectonics in the wedge*

Neotectonic activity within the exposed mountain front in the Darjiling Himalayas implies rejuvenation of a comparatively older and perhaps inactive part of the deforming Himalayan wedge. The questions that need to be asked are why does this occur? What are the deformation mechanisms that drive this? The details of the geometry and kinematics in the Darjiling Himalayan fold-and-thrust belt can only be worked out by detailed work in the entire deforming wedge. However, some first-order implications of the wedge-scale regional tectonics can be estimated from the observations made in this study. First, the development

Table 3
Thrust-related earthquake hypocenter data from the area between the exposures of the MBT and the Main Central Thrust in the central part of the Darjiling–Sikkim–Tibet wedge[a]

| Year | Date | Time | Latitude (north) | Longitude (east) | Depth (km) | Magnitude | Magnitude type |
|---|---|---|---|---|---|---|---|
| 1960 | 21 AUG | 03:29:04.90 | 27.0 | 88.5 | 29 | – | – |
| 1972 | 06 NOV | 10:56:15.00 | 27.1 | 88.2 | 33 | 4.8 | Body Wave (Mb) |
| 1975 | 23 JAN | 01:37:42.90 | 27.3140 | 88.255 | 33 | 4.8 | Mb |
| 1975 | 23 JAN | 01:37:42.63 | 27.4403 | 88.3712 | 33 | 4.5 | Mb |
| 1980 | 19 NOV | 19:00:47.60 | 27.2 | 88.7 | – | 6.8 | Mb |
| 1986 | 07 JAN | 20:20:00.36 | 27.3791 | 88.4265 | 41.5 | 4.7 | Mb |
| 1988 | 26 MAY | 16:30:05.50 | 27.4453 | 88.6069 | 42.1 | 4.7 | Mb |
| 1988 | 27 SEP | 19:10:10.7 | 27.175 | 88.293 | 33 | 5.0 | Mb |
| 1991 | 21 DEC | 19:52:45.5 | 27.904 | 88.139 | 57 | 4.9 | Mb |
| 1996 | 23 MAR | 16:07:34.20 | 27.167 | 88.3020 | 33 | 4.0 | Mb |
| 1996 | 13 SEP | 03:41:11.80 | 27.316 | 88.5383 | 33 | 4.1 | Mb |
| 1996 | 25 SEP | 17:41:13.50 | 27.36 | 88.59 | 25 | 5.1 | Mb |
| 1996 | 25 SEP | 17:41:17.54 | 27.602 | 88.8036 | 31.7 | 4.9 | Mb |
| 1998 | 18 MAR | 18:12:18.93 | 27.3680 | 88.3340 | 33 | 4.0 | Mb |
| 1998 | 10 SEP | 22:57:16.90 | 27.1990 | 88.3410 | 33 | 4.7 | Mb |

[a] Compiled from: http://www.isc.ac.uk/; http://quake.geo.berkeley.edu/ and http:// wwwneic.cr.usgs.gov/.

of the Kangmar antiform along a ramp in the basal decollement of the Himalayan fold-and-thrust belt caused the Himalayan wedge to become supercritical and caused progressive footwall imbrication extending the deformation in the wedge towards the foreland. It is unclear if the footwall imbrication produced progressively new active faults along with complete cessation of activity along the older thrusts or whether several of the imbricate faults were active at the same time. Nevertheless, an initial hinterland-to-footwall sequence of imbricate faults is likely to have been formed in response to the supercritical taper created at the back of the wedge by the formation of the Kangmar ramp antiform.

With the onset of the monsoon in the Late Miocene (Valdiya, 1999) and increased rates of erosion, the critically deforming wedge probably became subcritical and stalled over time. The high taper and strength of the back-end of the wedge was no longer sufficient to support further frontal imbrication especially because the middle part of the wedge (between MBT and MCT), which consisted of sheets carrying lower-strength sedimentary rocks, was excessively eroded. The wedge needed to restore critical taper, particularly in the middle part of the wedge where there is a drop in the material strength (basement to meta-sedimentary rocks), in order to advance into the Gangetic plain. Evidence of neotectonic activity within the exposed mountain front probably reflects deformation directed towards achieving this because duplex formation is one of the mechanisms for building taper in stalled, subcritical wedges (Boyer, 1995; Mitra 1997). However, in a zone where previous imbricate thrust faults are already present, formation of connective splays leading to the formation of connective splay duplexes (Mitra and Sussman, 1997) is the most likely mechanism of taper growth. It is also significant that most high magnitude, thrust-related earthquakes in the region have also been observed in the region between the MBT and the MCT (Table 3; Khattri, 1992) also pointing to probable taper building activities near the middle of the Darjiling–Sikkim–Tibet Himalayan wedge.

## 5. Conclusions

The Kalijhora area in the Darjiling Himalayas affords an excellent opportunity to study the effects of rejuvenation of thrust tectonics within a developed fold-and-thrust belt. Prior to the rejuvenation, the MBT was folded by a fault propagation fold that formed in front of the propagating, younger SKT. These folds were modified by rotation during the propagation and breakthrough of the SKT and motion along its footwall imbricates. The SKT thrust sheet (which included the folded MBT) was modified into its present configuration (Fig. 10e) by the formation of connecting splays and connecting splay duplexes in the hanging wall of the SKT (Fig. 10e). This caused the fault propagation antiform to become open and synform overturned with its limbs dipping southerly. Uplift related to the duplex formation also raised gravel beds on both banks of the Kalikhola stream and the river bed of the Tista causing it to pond and flood locally within the mountain front. Formation of connective splays and connective splay duplex in the hanging wall of the Andherijhora Thrust raised strath terraces along the west bank of Tista in the footwall of the SKT.

This study emphasises the need to look at the uplift of Quaternary river terraces and gravel beds in conjunction with the geometry and kinematics of the faults and rocks which they deform. It is hard to do that in front of the exposed mountain front because most thrusts are blind or have been covered by alluvium deposited by the rivers that flow out of the mountain front. Shallow seismic sections can help to a large extent in deciphering the causes for uplift of alluvial terraces and beds but the details of the kinematics could easily be mistaken. Typically, uplift of alluvial and river terraces have been interpreted to be the result of fault activity in the subsurface. However, it could easily be the result of passive folding as seen in this study. Therefore, an integrated look at the palaeo- and the neotectonic evidence must become the norm for understanding the deformation in active mountain belts like the Himalayas.

## Acknowledgements

This work was funded by Department of Science and Technology (DST), India, Grant No. ESS/CA/A9-49/97 & C-MMACS. Excellent critical reviews by J.-L. Mugnier, Wanda Taylor, and K. S. Valdiya were instrumental in greatly improving the quality of this paper. I also thank JSG Associate Editor Richard Norris for his comments and help in improving the quality of this paper. The work is partly an outgrowth of the short course 'Active Tectonics and Paleoseismology' organised by the DST, Centre for Earth Science Studies (CESS), Trivandrum, and Jawaharlal Nehru Centre for Advanced Research (JNCAR), Bangalore in 1998 where the author was a participant. I thank Krishnapriya Basak for her able assistance in the field. I also benefited from discussions and comments from Kusala and C. P. Rajendran, D. Mukhopadhyay, Gautam Mitra, Abdul Matin and Krishnapriya Basak. Rick Allmendinger's Stereoplot was used to construct the stereoplots used in this paper.

## References


Acharyya, S.K., 1976. On the nature of the Main Boundary Fault in the Darjiling sub-Himalaya. Geological Survey of India Miscellaneous Publications 24, 395–408.

Acharyya, S.K., 1994. The Cenozoic Foreland Basin and tectonics of the eastern sub-Himalaya: problems and prospects. Himalayan Geology 15, 3–21.

Acharyya, S.K., Sastry, M.V.A., 1976. Stratigraphy of the eastern Himalaya. Geological Survey of India Miscellaneous Publications 41, 49–64.

Acharyya, S.K., Dutta, A.K., Sastry, M.V.A., 1976. Siwalik stratigraphy and its bearing on the Main Boundary Fault. Geological Survey of India Miscellaneous Publications 41, 67–79.

Adams, J., 1980. Active tilting of the United States mid-continent; geodetic and geomorphic evidence. Geology 8, 442–446.

Boyer, S.E., 1995. Sedimentary basin taper as a factor controlling the geometry and advance of thrust belts. American Journal of Science 295, 1220–1254.

Boyer, S.E., Elliott, D., 1982. Thrust systems. American Association of Petroleum Geologists Bulletin 66, 1196–1230.

Brown, L.D., Zhao, W., Nelson, K.D., Hauck, M., Alsdorf, D., Ross, A., Cogan, M., Clark, M., Xianwen, L., Che, J., 1996. Bright spots, structure, and magmatism in southern Tibet from INDEPTH Seismic Reflection Profiling. Science 274, 1688–1690.

Burnett, A.W., Schumm, S.A., 1983. Alluvial-river response to neotectonic deformation in Louisiana and Mississippi. Science 222, 49–50.

Chakraborty, S., Chakraborty, S.K., 1989. Origin and evolution of the Kalijhora Point Bar on Tista River, Darjiling District, West Bengal. Journal of Geological Society of India 33, 583–587.

Chalaron, E., Mugnier, J.L., Mascle, G., 1995. Control of thrust tectonics in the Himalayan foothills: a view from a neotectonic model. Tectonophysics 248, 139–163.

Chapple, W.M., 1978. Mechanics of thin-skinned fold-and-thrust belts. Geological Survey of America Bulletin 89, 1189–1198.

Dahlen, F.A., 1984. Noncohesive critical coulomb wedges: an exact solution. Journal of Geophysical Research 89 (10), 125–133.

Dahlstrom, C.D.A., 1970. Structural geology in the eastern margin of the Canadian Rocky Mountains. Bulletin of Canadian Petroleum Geology 18, 332–406.

Davis, D., Suppe, J., Dahlen, F.A., 1983. Mechanics of fold and thrust belts and accretionary wedges. Journal of Geophysical Research 88 (B2), 1153–1172.

DeCelles, P.G., Mitra, G., 1995. History of the Sevier orogenic wedge in terms of critical taper models, north east Utah and south west Wyoming. Geological Society of America Bulletin 107, 454–462.

Elliott, D., 1976. The motion of thrust sheets. Journal of Geophysical Research 81, 949–963.

Emmerman, S.H., Turcotte, D.L., 1983. A fluid model for the shape of accretionary wedges. Earth and Planetary Science Letters 63, 379–384.

Khattri, K.N., 1992. Seismological investigations in north eastern region of India. Memoir Geological Society of India 23, 275–302.

King, G., Bailey, G., Sturdy, D., 1994. Active tectonics and human survival strategies. Journal of Geophysical Research 99, 20063–20078.

Kumar, R., 1988. Fundamentals of Historical Geology and Stratigraphy of India. Wiley Eastern Limited, New Delhi.

Le Fort, P., 1975. Himalayas: the collided range. Present knowledge of the continental arc. American Journal of Science 275A, 1–44.

Lyon-Caen, H., Molnar, P., 1983. Constraints on the structure of the Himalaya from an analysis of gravity anomalies and a flexure model of the lithosphere. Journal of Geophysical Research 88, 8171–8191.

McNaught, M.A., Mitra, G., 1993. A kinematic model for the origin of footwall synclines. Journal of Structural Geology 16, 493–503.

Medlicott, H.B., 1864. On the geological structure and relations of the southern portion of the Himalayan ranges between the Rivers Ganges and the Ravee. Memoir Geological Survey of India 3, 102.

Mitra, G., Sussman, A., 1997. Structural evolution of connecting splay duplexes and their implications for critical taper: an example based on geometry and kinematics of the Canyon Range culmination, Sevier Belt, central Utah. Journal of Structural Geology 19, 503–521.

Mitra, G., 1997. Evolution of salients in a fold-and-thrust belt: the effects of sedimentary basin geometry, strain distribution and critical taper. In: Sengupta, S. (Ed.), Evolution of Geologic Structures from Macro- to Micro-scales. Chapman and Hall, London, pp. 59–90.

Mitra, S., 1990. Fault-propagation folds: geometry, kinematic evolution, and hydrocarbon traps. American Association of Petroleum Geologists Bulletin 74, 921–945.

Molnar, P., 1990. A review of the seismicity and the rates of active underthrusting and deformation at the Himalaya. Journal of Himalayan Geology 1 (2), 131–154.

Molnar, P., Brown, E.T., Burchfiel, B.C., Qidong, D., Xianyue, F., Jun, L., Raisbeck, G.M., Jianbang, S., Zhangming, W., Yiou, F., Huichuan, Y., 1994. Quaternary climate change and formation of river terraces across growing anticlines on the northern flank of the Tien Shan. Journal of Geology 102, 583–602.

Mugnier, J.L., Huyghe, P., Chalaron, E., Mascle, G., 1994. Recent movements along the Main Boundary Thrust of Himalayas: normal faulting in an overcritical wedge? Tectonophysics 238, 199–215.

Nakata, T., 1989. Active faults of the Himalaya of India and Nepal. Geological Society of America Special Paper 232, 243–264.

Nelson, K. D. and 26 others, 1996. Partially molten middle crust beneath southern Tibet: synthesis of Project INDEPTH results. Science 274, 1684–1688.

Ni, J., Barazangi, M., 1984. Seismotectonics of the Himalayan collision zone: geometry of the underthrusting Indian plate beneath the Himalaya. Journal of Geophysical Research 89 (B2), 1147–1163.

Ouchi, S., 1985. Response of alluvial rivers to slow active tectonic movement. Geological Society of America Bulletin 96, 504–515.

Powell, C.McA., 1979. A speculative tectonic history of Pakistan and surroundings: some constraints from the Indian Ocean. In: Farah, A., DeJong, K. (Eds.), Geodynamics of Pakistan. Geological Survey of Pakistan, Quetta, pp. 5–24.

Raiverman, V., 1997. On dating of the Himalayan Thrusts. Himalayan Geology 18, 63–79.

Roy, K.K., 1976. Some problems of stratigraphy and tectonics of the Darjiling and Sikkim Himalayas. Geological Survey of India Miscellaneous Publications 24 (2), 379–394.

Russ, D.R., 1982. Style and significance of surface deformation in the vicinity of New Madrid, Missouri. U.S. Geological Survey Professional Paper 1236-H, 95–114.

Schumm, S.A., 1986. Alluvial river response to active tectonics. In: Active Tectonics: Studies in Geophysics. National Academic Press, Washington, DC, pp. 80–94.

Schwan, W., 1980. In: Saklani, P.S. (Ed.), Shortening Structures in Eastern and North-western Himalayan Rocks. Today and Tomorrow's Printers and Publishers, New Delhi.

Seeber, I., Armbruster, J., 1981. Great detachment earthquakes along the Himalayan arc and long-term forecasting. In: Simpson, D.W., Richards, P.G. (Eds.), Earthquake Prediction: an International Review. American Geophysical Union 4, Maurice Ewing Series, pp. 259–277.

Srivastava, P., Mitra, G., 1994. Thrust geometries and deep structure of the outer and lesser Himalayas, Kumaon of the Himalayan fold-and-thrust belt. Tectonics 13, 89–109.

Stockmal, G.S., 1983. Modeling of large-scale accretionary wedge formation. Journal of Geophysical Research 88, 8271–8287.

Tator, B.A., 1958. The aerial photograph and applied geomorphology. Photogrametric Engineering 24, 549–561.

Valdiya, K.S., 1998. Dynamic Himalaya. Universities Press, Hyderabad.

Valdiya, K.S., 1999. Rising Himalaya: advent and intensification of monsoon. Current Science 76 (4), 514–524.

Wadia, D.N., 1975. Geology of India: Tata. McGraw Hill, New Delhi.

Welch, D.M., 1973. Channel form and bank erosion, Red River, Manitoba. 9th Hydrology Symposium, Edmonton. Abstracts of proceedings, University of Alberta, Canada.

Willett, S.D., 1992. In: McClay, K.R. (Ed.), Dynamic and Kinematic Growth and Change of a Coulomb Wedge. Chapman and Hall, New York, pp. 19–31.

Williams, C.A., Connors, C., Dahlen, F.A., Price, E.J., Suppe, J., 1994. Effect of the brittle-ductile transition on the topography of compressive mountain belts on Earth and Venus. Journal of Geophysical Research 99 (19), 947–974.

Yeats, R.S., Nakata, T., Farah, A., Fort, M., Mirza, M.A., Pandey, M.R., Stein, R.S., 1992. The Himalayan Frontal Fault System. Annales Tectonicae (Special Issue Suppl.) VI, 85–98.